Neuroscience 210 (2012) 431–441

THE DOSE-RESPONSE EFFECT OF ACUTE INTRAVENOUS TRANSPLANTATION OF HUMAN UMBILICAL CORD BLOOD CELLS ON BRAIN DAMAGE AND SPATIAL MEMORY DEFICITS IN NEONATAL HYPOXIA-ISCHEMIA

S. DE PAULA,[a] S. GREGGIO,[a] D. R. MARINOWIC,[b] D. C. MACHADO[b] AND J. COSTA DACOSTA[a]*

[a]*Laboratório de Neurociências e de Sinalização Celular, Instituto do Cérebro, Pontifícia Universidade Católica do Rio Grande do Sul (PUCRS), Porto Alegre, RS, Brazil*

[b]*Laboratório de Biologia Celular e Molecular, Instituto de Pesquisas Biomédicas, Pontifícia Universidade Católica do Rio Grande do Sul (PUCRS), Porto Alegre, RS, Brazil*

Abstract—Despite the beneficial effects of cell-based therapies on brain repair shown in most studies, there has not been a consensus regarding the optimal dose of human umbilical cord blood cells (HUCBC) for neonatal hypoxia-ischemia (HI). In this study, we compared the long-term effects of intravenous administration of HUCBC at three different doses on spatial memory and brain morphological changes after HI in newborn Wistar rats. In addition, we tested whether the transplanted HUCBC migrate to the injured brain after transplantation. Seven-day-old animals underwent right carotid artery occlusion and were exposed to 8% O_2 inhalation for 2 h. After 24 h, randomly selected animals were assigned to four different experimental groups: HI rats administered with vehicle (HI+vehicle), HI rats treated with 1×10^6 (HI+low-dose), 1×10^7 (HI+medium-dose), and 1×10^8 (HI+high-dose) HUCBC into the jugular vein. A control group (sham-operated) was also included in this study. After 8 weeks of transplantation, spatial memory performance was assessed using the Morris water maze (MWM), and subsequently, the animals were euthanized for brain morphological analysis using stereological methods. In addition, we performed immunofluorescence and polymerase chain reaction (PCR) analyses to identify HUCBC in the rat brain 7 days after transplantation. The MWM test showed a significant spatial memory recovery at the highest HUCBC dose compared with HI+vehicle rats ($P<0.05$). Furthermore, the brain atrophy was also significantly lower in the HI+medium- and high-dose groups compared with the HI+vehicle animals ($P<0.01$; 0.001, respectively). In addition, HUCBC were demonstrated to be localized in host brains by immunohistochemistry and PCR analyses 7 days after intravenous administration. These results revealed that HUCBC transplantation has the dose-dependent potential to promote robust tissue repair and stable cognitive improvement after HI brain injury.

Key words: stem cells, hypoxia-ischemia, asphyxia, cord blood stem cell transplantation, dose-response relationship.

The hypoxia-ischemia (HI) that occurs during the neonatal period is an important cause of mortality and severe neurologic morbidity in children, affecting approximately 1 to 3 cases per 1000 full-term live births in developed countries (Wyatt et al., 2007). Approximately 50% of infants with severe HI die, and up to 25% of survivors have long-term disabilities, such as epilepsy, cerebral palsy, and cognitive impairments (Ferriero, 2004). Despite technological and scientific advances in the perinatal care of at-risk newborns, until recently, the management of newborn infants with HI has been limited to supportive care in the neonatal intensive care unit. Consequently, new neuroprotective strategies have been investigated in experimental studies and clinical trials because of the clinical relevance and socioeconomic impact generated by neonatal brain damage. However, with the exception of hypothermia, which shows satisfactory outcomes in infants with mild or moderate HI injury, these therapies have limited results (Sahni and Sanocka, 2008; Johnston et al., 2011). As a result, cell based-therapy has been proposed as a novel treatment approach for severe neurological diseases, including HI. In the neonatal context, obtaining stem cells from umbilical cord blood offers low risk or discomfort to the newborn, and the cells can be transplanted after autologous collection. In addition, umbilical cord blood can be used therapeutically during the perinatal period or can be cryopreserved for later use (Santner-Nanan et al., 2005; Harris, 2008; Liao et al., 2011).

Current investigations using different cell dosages, delivery routes, and types of human umbilical cord blood cells (HUCBC) have reported that this therapy is neuroprotective in most animal models of neonatal brain injury (Meier et al., 2006; Pimentel-Coelho et al., 2009; Yasuhara et al., 2010; Rosenkranz et al., 2010; Xia et al., 2010). Although these preclinical studies have demonstrated promising results for brain damage, we have recently shown in a rat model of severe neonatal HI that a single dose of 1×10^7 transplanted HUCBC can migrate to the brain after intravenous injection but does not improve the cognitive and morphological outcomes 3 weeks post-transplantation (de Paula et al., 2009). These previous data demonstrated that several variables will need to be explored to optimize the use of cell therapy in children with HI brain damage, including aspects such as timing, route of transplantation,

*Corresponding author. Tel: +5551-33203250; fax: +5551-33203312.
E-mail address: jcc@pucrs.br (J. Costa DaCosta).

Abbreviations: ANOVA, analysis of variance; DAPI, 4',6-diamidino-2-phenylindole dihydrochloride; HI, hypoxia-ischemia; HUCBC, human umbilical cord blood cells; HuNu, human nuclei-positive cells; MWM, Morris water maze; PCR, polymerase chain reaction; PND, postnatal day; SEM, standard error of the mean.

0306-4522/12 $36.00
10.1016/j.neuroscience.2012.03.009

cellular type, and dosage (Bliss et al., 2007; Janowski et al., 2010).

One of the most important questions in terms of efficacy and tolerance for the clinical approach of stem cell treatment is the number of administered cells (Wechsler et al., 2009). Some reports have assessed the dose-response association between cell concentration and the functional effects of the treatment on animal models of heart damage (Iwasaki et al., 2006; Wolf et al., 2009). However, there are insufficient data showing the relationship between cell dose and long-term neurological outcomes (Vendrame et al., 2004; Garbuzova-Davis et al., 2008; Omori et al., 2008; Stroemer et al., 2009; Yang et al., 2011), and there are no dose-ranging studies in neonatal HI. Hence, we conducted a pioneer investigation to compare the effect of intravenous administration of HUCBC at three different doses on spatial memory and brain morphological changes in 60-day-old rats previously subjected to neonatal HI. In addition, we tested whether the transplanted HUCBC migrate to the injured brain 7 days after intravenous administration.

EXPERIMENTAL PROCEDURES

Animals

All experimental procedures were performed in accordance with the NIH Guide for the Care and Use of Laboratory Animals and were approved by the Animal Care and Ethics Committee of Pontifícia Universidade Católica do Rio Grande do Sul, RS, Brazil (CEP 09/04761). A total of 50 male Wistar rats were kept under a constant 12:12-h light–dark cycle at room temperature (23±1 °C), with free access to food and water. After each normal delivery, the litter sizes were adjusted to eight pups per litter. Pups were kept with their dams until weaning at postnatal day (PND) 21. Efforts were made to minimize animal suffering and to reduce the number of animals used.

Experimental groups

The animals were randomly assigned to five experimental groups ($n=10$ each): sham-operated rats, rats administered with vehicle (HI+vehicle), and rats with 1×10^6 (HI+low-dose), 1×10^7 (HI+medium-dose), or 1×10^8 (HI+high-dose) HUCBC transplanted into the jugular vein 24 h post-HI. The rat pups from each litter were randomly divided among the five experimental groups to avoid "litter effects" on the results of brain injury and cognitive performance. Only male rats were used in our study. An additional cohort of HI animals was injected with HUCBC as described earlier in the text but was euthanized 7 days after transplantation. In these animals, brain samples were collected for immunofluorescence staining and PCR analyses. All experiments were performed by blinded investigators.

Hypoxic-ischemic model

In this study, we used the Levine rat model, modified by Rice et al (Rice et al., 1981) for neonatal rats. On PND 7 (weights ranging from 12 to 15 g), each animal was briefly anesthetized with halothane delivered by a face mask. The right common carotid artery was identified through a midline longitudinal neck incision, isolated from the vagus nerve, and permanently double-ligated with a 7.0 surgical silk suture. The entire surgical procedure was completed within 15 min. After the wounds were sutured, the animals were put back into their cages and allowed to recover for 2–4 h in the company of their dams. The rats were then placed in a hypoxia chamber for 2 h, with a constant flow of humidified 8% oxygen balanced with nitrogen. The hypoxia chamber was kept in a water bath to maintain the ambient temperature inside the chamber at a normal range (37–38 °C). After hypoxic exposure, the pups were returned to their dams for recovery. The sham-operated animals underwent anesthesia and incision only.

HUCBC preparation and intravenous administration

After obtaining informed consent, HUCBC were collected *ex-utero* from healthy volunteers using sterile syringes containing 5.000 UI of heparin, immediately after full-term delivery. We have used a proportion of one donated umbilical cord to 4–7 transplanted rats, depending on the amount of available mononuclear cells. Blood samples were kept at a temperature of 4 °C during the transport and storage procedures, and all units were processed within 24 h after collection. For the separation of mononuclear cells, the obtained material was diluted in RPMI-1640 medium (1:1) (Gibco, Grand Island, NY, USA). The cells were resuspended and fractionated on a density gradient generated by centrifugation, over Ficoll-Paque solution with a density of 1.077 g/L (Histopaque 1077, Sigma Aldrich, St. Louis, MO, USA), at $400\times g$ for 30 min at 25 °C. The mononuclear fraction over the Ficoll-Paque layer was collected and washed twice with Dulbecco's Phosphate Buffered Saline (DPBS) (Gibco, Grand Island, NY, USA). The cell density was determined with a Neubauer-counting chamber, and the number of viable cells was determined using the Trypan Blue 0.4% exclusion method. For the detection of surface antigens, HUCBC were incubated with fluorescein isothiocyanate- (FITC) or phycoerythrin- (PE) conjugated monoclonal antibody against CD45 (hematopoietic precursor cells), CD105 (bone marrow precursor cells), CD34 (hematopoietic and endothelial precursor cells), and CD117 (hematopoietic precursor cells) (Becton Dickinson Biosciences, San Jose, CA, USA). Labeled cells were collected and analyzed using a FACSCalibur flow cytometer (BD Biosciences, Franklin Lakes, NJ, USA). Twenty-four hours after HI, animals weighting approximately 20 g received HUCBC (1×10^6, 1×10^7, or 1×10^8 cells resuspended in saline) or vehicle delivered into the left jugular vein using an ultrafine insulin syringe with a 31-gauge needle in a volume of 100 μl. For that procedure, animals were anesthetized with halothane, the previous neck suture was carefully opened, and the left external jugular vein was isolated from adjacent tissue to facilitate the intravenous injection. Thereafter, the skin was once again closed with suture, and the animals were returned to their dams for recovery.

Spatial version of the Morris water maze task

Spatial memory performance was evaluated 8 weeks after HI exposure or sham operation using the Morris water maze (MWM) as previously described (Greggio et al., 2011; Venturin et al., 2011). The water maze consisted of a black circular pool (200 cm in diameter) conceptually divided into four equal imaginary quadrants. The water temperature was maintained at 21–24 °C. Two centimeters beneath the surface of the water and hidden from the rat's view was a black circular platform (15 cm in diameter). The water maze was located in a well-lit white room, and cues were placed on the walls around the pool, which could be used by the rats for spatial orientation. Training on the spatial version of the MWM was performed over five consecutive days. On each day, the rats received eight training trials during which the hidden platform was kept at a constant location. The movements of the animals were monitored during the sessions with a video camera fixed to the ceiling over the center of the maze. A different starting location was used in each trial, which consisted of a swim followed by a 30-s platform sit. The rats that did not find the platform within 60 s were guided to it by the experimenter. To assess long-term memory, 24 h after the final trial, the platform was removed from the maze and the parameters measured were (1) the percentage

of time spent in the target quadrant and (2) the latency to reach the original platform position.

Brain morphological study

After completing behavioral tests, the animals were deeply anesthetized with a ketamine and xylazine mixture (90:10 mg/ml; i.p.) and perfused transcardially with saline followed by 4% paraformaldehyde, pH 7.4. The brains were removed from the skulls, post-fixed in the same solution at room temperature for 24 h, and cryoprotected by immersion in a 30% sucrose solution in phosphate buffer at 4 °C until they sank. The brains were then quickly frozen in isopentane that was cooled in liquid nitrogen (−70 °C). Coronal sections of the brains (50 μm) were cut using a cryostat (Shandon, UK), collected at equidistant intervals, and stained with Cresyl Violet using the Nissl method. The cerebellum was excluded from the study. Digitized images of the coronal sections overlaid on a point counting grid were obtained with a high-performance CCD camera installed on a stereoscopic light microscope (DF Vasconcellos MU-M19, Brazil), interfaced with Image Pro Plus 6.1. (Media Cybernetics, Silver Spring, MD, USA), and run on a personal computer. Images of the hemispheres were displayed on a high-resolution video monitor, and the boundaries were defined in accordance with the Paxinos and Watson atlas (Paxinos and Watson, 1986). The Cavalieri method was used to estimate the hemispheric volume by the summation of points multiplied by the distance between sections. With the coronal sections displayed on the point counting grid, we counted the number of points hitting the hemisphere. Volume estimation was performed in 10 equally spaced sections for each rat brain in the affected and control hemispheres. The number of points counted was used for the estimation of hemispheric volume (mm^3) using the following equation: V=T.a/p.ΣP, where V=volume estimation; T=distance between the analyzed sections (1200 μm); a/p=point area (1 mm^2); and ΣP=the sum of points overlaid in the image (Galvin and Oorschot, 2003; Alles et al., 2010). Besides, to evaluate the extent of brain injury, we calculated the percentage of brain tissue loss in the ipsilateral hemisphere (left hemisphere—residual ipsilateral hemisphere divided by left hemisphere× 100%), as previously described (You et al., 2007).

Immunofluorescent staining and confocal laser scanning

Migration of HUCBC was performed in low-, medium-, and high-dose groups using the indirect immunofluorescence method. Seven days after intravenous HUCBC transplantation, a subgroup of HI animals (n=6) was anesthetized with a ketamine and xylazine mixture (90:10 mg/ml; i.p.) and perfused transcardially first with a saline solution containing heparin, followed by 4% paraformaldehyde in 0.1 M phosphate-buffered saline (PBS), pH 7.4. The brains were removed, post-fixed in 4% paraformaldehyde, and then processed for paraffin sectioning. A series of four 15-μm thick coronal sections containing the cortex and hippocampus were cut with a microtome. After being deparaffinized, the sections were placed in boiling Target Unmasking Fluid solution (TUF; PanPath, Amsterdam, NL) in a microwave oven for 10 min. After cooling at room temperature, nonspecific protein binding was blocked with 2.5% albumin serum bovine (Sigma Aldrich, St. Louis, MO, USA) for 1 h. For the detection of the grafted human stem cells, the coronal slices were incubated overnight at 4 °C with a primary mouse anti-human nuclear antigen monoclonal antibody (HuNu) (1:100; Chemicon, Temecula, CA, USA). The sections were then washed with 0.1 M PBS and incubated with Alexa Fluor 488 goat anti-mouse IgG (H+L) secondary antibody (1:1.000; Invitrogen, Carlsbad, CA, USA) at 37 °C in the absence of light for 1 h. Glass coverslips were mounted using ProLong Gold antifade mounting medium with 4',6-diamidino-2-phenylindole dihydrochloride (DAPI) Invitrogen (Carlsbad, CA, USA) to visualize cell nuclei. Reactivity of the antibody was confirmed in positive samples and negative control sections. Colocalization of DAPI with the human-specific marker HuNu was detected, analyzed, and photographed qualitatively using a confocal laser scanning microscope (LSM 5 Exciter, Carl Zeiss, Germany) coupled to a Pro-Series High Performance CCD camera and Zen 5.0 software (Carl Zeiss, Inc.). Blue (DAPI) and green (Alexa 488 for HuNu) fluorochromes in the slices were excited by a laser beam at 405 nm (Diode) and 488 nm (argon), and the emissions were sequentially acquired with two separate photomultiplier tubes through LP 420- and BP 505–530-nm emission filters, respectively. The areas of interest were scanned with a pinhole under each laser, set to a value of 1.0 Airy unit for the×63 oil immersion objective lens (Plan-Neofluar, NA=1.4). The scanning dimensions were 1024×1024 pixels, and the specimens were scanned an average of four times with a 12-bit pixel depth. The Z-stacks (±15 optical slices) were obtained at a thickness of 1 μm, and colocalization was evaluated in single optical planes taken through the entire z-axis of each cell. Only $HuNu^+$ cells contained entirely within the three dimensions of a stack were included in the analysis.

Polymerase Chain Reaction (PCR analysis

An additional group of HI rats (n=7) was euthanized, and samples were collected 7 days after HUCBC intravenous injection. DNA was obtained from the rat brains using the phenol/chloroform method described by Isola et al (Isola et al., 1994). PCR analysis was performed to identify the presence of administrated HUCBC in the brains of transplanted animals using complementary primers to the human β-actin gene sequence. We used the forward primer 5′-TCCCTGTACGCCTCTGGCCATA-3′ and the reverse primer 5′-CCTTCTGCATCCTGTTGGTGATGCTA-3′ complimentary to the human β-globin DNA sequence and reamplified with the forward primer 5′-TGACTGGCCGGAACCTGACT-3′ and the reverse primer 5′-GGTGATGACCTGGCCATTGGG-3′ using the nested PCR technique, resulting in fragments of 535 and 209 bp, respectively. The positive control (DNA from human peripheral blood) and negative control (without any DNA) samples were assayed along with experimental samples in every reaction. Amplified products were detected by gel electrophoresis (2% agarose containing ethidium bromide) for 30 min, at a voltage of 100 V and an amperage of 400 mA. The gels were visualized under an ultraviolet transilluminator (3UV™), and the images were captured using photodocumentation equipment connected to Quantity One software (Bio-Rad, CA, USA).

Statistical analysis

Statistical analysis was performed using the PrismGraph 5.0 program (GraphPad Software, San Diego, CA, USA). The variables are presented as the means±standard error of the mean (SEM). Behavioral and morphological outcomes were compared between the groups using one-way analysis of variance (ANOVA) followed by post-hoc Dunnett's or Bonferroni's tests, as appropriate. Pearson's correlation coefficient and linear regression analysis between the variables were calculated. Data were considered significantly different if $P<0.05$.

RESULTS

HUCBC characterization

To determine the phenotypic characteristics of mononuclear cells derived from human umbilical cord blood, four fluorescence-activated cell sorting (FACS) analyses were used to examine the expression of cell-surface marker (Fig. 1A–D). In brief, 2.4% of the cells expressed CD34,

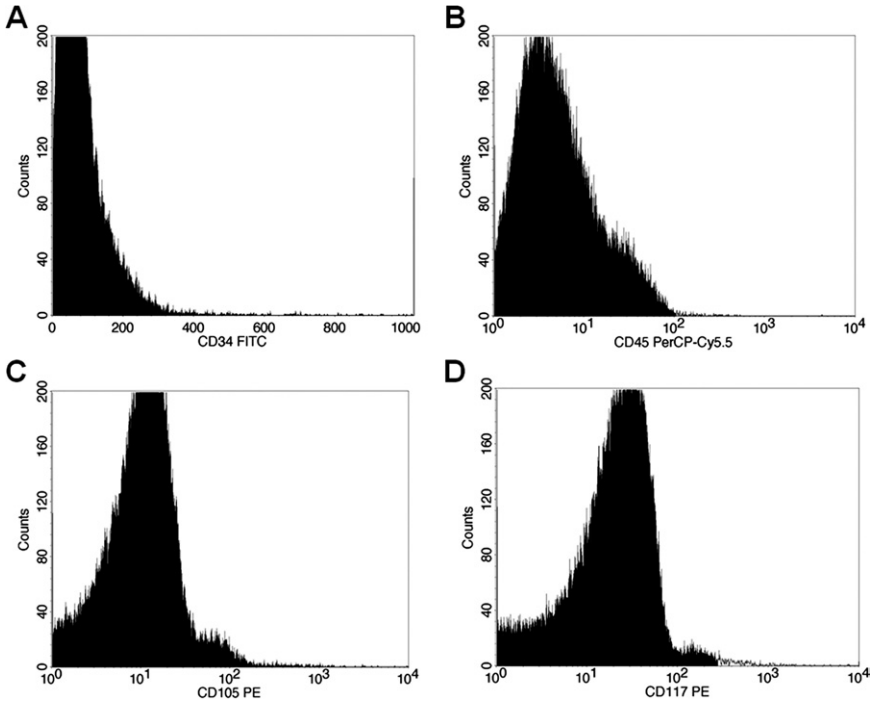

Fig. 1. Immunophenotypic analysis of mononuclear fraction derived from human umbilical cord blood. The histograms show the fluorescence intensity of HUCBC reacting with (A) CD34, (B) CD45, (C) CD105, and (D) CD117 during flow cytometry. A total of 5000 events were considered for each analysis.

23.14% expressed CD45, 50.41% expressed CD105, and 71.25% expressed CD117. Taken together, the data showed that the isolated cord blood cells exhibited a mixture of different cellular types, consistent with the literature (Mayani and Lansdorp, 1998; Park et al., 2009; Ruhil et al., 2009).

A high dose of HUCBC transplanted intravenously rescues long-term spatial memory impairments in hypoxic-ischemic rats

To assess the effects of three different doses of HUCBC on long-term spatial memory deficits, we employed the MWM task. The mean escape latencies to the hidden platform were shortened as training progressed, and the groups showed a different rate of change over time [$F_{(4,\ 220)}=1.10$, $P=0.34$, Fig. 2A]. As shown in Table 1, Bonferroni post hoc test showed a significant difference ($P<0.001$) between the HI+vehicle and sham groups throughout the entire 5-day training session. Only the group of HI animals that were administered with the highest HUCBC dose presented learning similarity to sham rats and a significant difference to HI+vehicle group. Besides, there were no statistical differences in the training performance among the transplanted groups. The probe test was performed 24 h after the last training session in the absence of the escape platform, and HI+vehicle rats exhibited significant spatial memory deficits. One-way ANOVA followed by Dunnett's test indicated that the escape latency to swim over the previous position of the escape platform was longer in the HI+vehicle group (37.66±6.99 s) than in the sham group (7.89±1.19 s) ($P<0.01$) (Fig. 2B). Among treatment groups, only the HI+high dose of HUCBC had a markedly shorter time required to reach the platform location (16.86±3.48 s) ($P<0.05$ vs. HI+vehicle). For the second analyzed variable, the HI+vehicle group spent less time swimming in the target quadrant that previously contained the escape platform (32.97±3.91%) compared with either the sham-operated (62.52±4.17%) ($P<0.001$) or HI+high-dose groups (48.17±2.93%) ($P<0.05$) (Fig. 2C). No significant differences were observed for either variable when HI+low- and medium-dose animals were compared with HI+vehicle animals, suggesting that only a high dose of HUCBC rescues the learning and memory impairments.

Intravenously transplanted HUCBC dose-dependently prevent brain lesions after neonatal hypoxia-ischemia in rats

Absolute hemispheric volume analysis showed significant atrophy of the hemisphere ipsilateral to the carotid occlusion (right side) in the HI+vehicle group when compared with the contralateral hemisphere (296.76±74.23 vs. 605.28±47.39 mm^3; $P<0.001$) (Fig. 3A). Similarly, the HI+low-dose group also had a significantly reduced volume of the right hemisphere compared with the left one (451.92±64.82 vs. 639.12±17.14 mm^3; $P<0.05$). No difference was observed between the right and left hemispheres in sham animals (641.40±7.49 vs. 658.92±6.23 mm^3) or in the HI groups that received only medium (560.16±63.65 vs. 664.56±16.74 mm^3) or high doses (658.20±22.32 vs. 658.56±18.75 mm^3) of HUCBC. As shown in Fig. 3B, we also examined cerebral atrophy in terms of the percentage of brain tissue loss, which was calculated using the contralateral (left, non-ischemic)

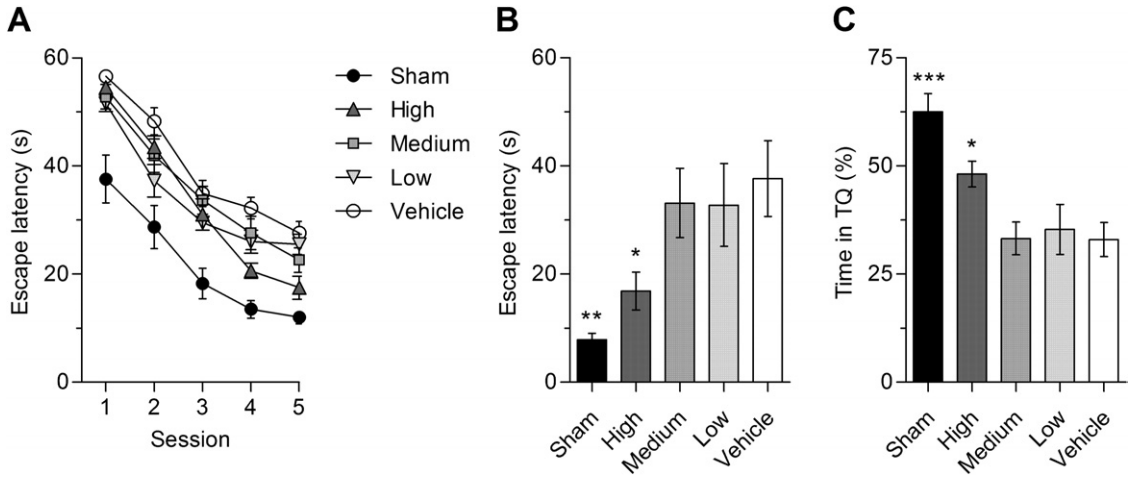

Fig. 2. A high dose of HUCBC transplantation resulted in a significant attenuation of injury-induced spatial memory impairment in hypoxic-ischemic rats. (A) The mean escape latencies to the hidden platform were obtained from a 5-d training session. Data are presented in blocks of eight trials as mean±SEM. (B) The sham-operated and HI+high-dose (1×10^8 cells) groups showed a significantly faster latency of swimming over the previous platform location when compared with HI+vehicle animals. (C) The sham-operated and HI+high-dose groups spent a greater percentage of time searching the quadrant in which the platform had been submerged during training compared with HI+vehicle rats. No significant differences were observed when low- or medium-dose groups were compared with the HI+vehicle group for either variable. The values were presented as the mean±SEM; $n=10$ per group. Differences between groups were analyzed by one-way ANOVA followed by the Dunnett post hoc test; * $P<0.05$, ** $P<0.01$, and *** $P<0.001$ vs. HI+vehicle.

hemisphere as a control. One-way ANOVA followed by Dunnett's test indicated that the percentage of damage in the HI+vehicle group (54.90±9.16%) was markedly higher than in the sham-operated group (3.09±0.60%; $P<0.001$). However, the right hemispheric volume loss caused by HI was significantly lower in rats of the medium-dose (18.29±8.79%; $P<0.01$) and high-dose (3.21±0.84%; $P<0.001$) groups when compared with vehicle-treated animals, suggesting a protective dose-dependent effect. There was no statistically significant difference between the HI+vehicle and low-dose groups (29.70±9.89%). Representative samples of Nissl staining from the brain hemispheres of rats after HI insult are shown in Fig. 3C. Examination of brain tissues showed vast ischemic damage with extensive atrophy and the formation of porencephalic cysts in the ipsilateral hemisphere of the HI+vehicle rats. Additionally, we observed a positive linear relation between the degree of hemispheric tissue volume loss and the escape latency of the MWM probe trial when all groups were pooled for correlation analysis ($R=0.71$, $P<0.0001$, Fig. 4A). Besides, a negative correlation between the degree of hemispheric tissue volume loss and the time spent in the target quadrant of the MWM probe trial was detected ($R=-0.57$, $P<0.0001$, Fig. 4B). Taken together, these findings suggest that neonatal HI-induced brain injury contributes to spatial learning and memory deficits in rats, and that HUCBC dose-dependently hinders brain lesion and cognitive impairments due to neonatal HI.

HUCBC are detected in the rat brain 7 days post-transplantation as determined by PCR analysis and immunofluorescence staining

Additional groups of HI rats were euthanized 7 days after HUCBC transplantation for human cell detection in host rat brains using an anti-human nuclear antibody. Double-stained sections were examined using a confocal laser scanning microscope to identify human nuclei-positive cells (HuNu) that colabeled with DAPI. Most of the surviving human cells were located in the cortex and the hip-

Table 1. Morris water maze acquisition performance

Groups	Training session				
	1	2	3	4	5
Sham	37.6±4.4***	28.7±4.0***	18.3±2.8***	13.5±1.6***	12.0±1.2***
Vehicle	56.6±0.9†††	48.3±2.5†††	34.9±2.4†††	32.2±2.0†††	27.6±2.1†††
Low	51.6±1.5†††	37.3±3.0**	29.5±1.0††	26.0±2.1††	25.5±1.9†††
Medium	52.8±2.3†††	41.9±3.1†††	33.7±2.6†††	27.6±3.1†††	22.6±2.3†
High	54.5±1.0†††	43.5±2.1†††	31.0±2.9††	20.6±1.4**	17.5±2.1*

Values represent the mean±SEM ($n=10$ rats/group).
* $P<0.05$, ** $P<0.01$, and *** $P<0.001$ vs. vehicle group; † $P<0.05$, †† $P<0.01$, and ††† $P<0.001$ vs. sham group in Bonferroni post hoc test after two-way ANOVA.

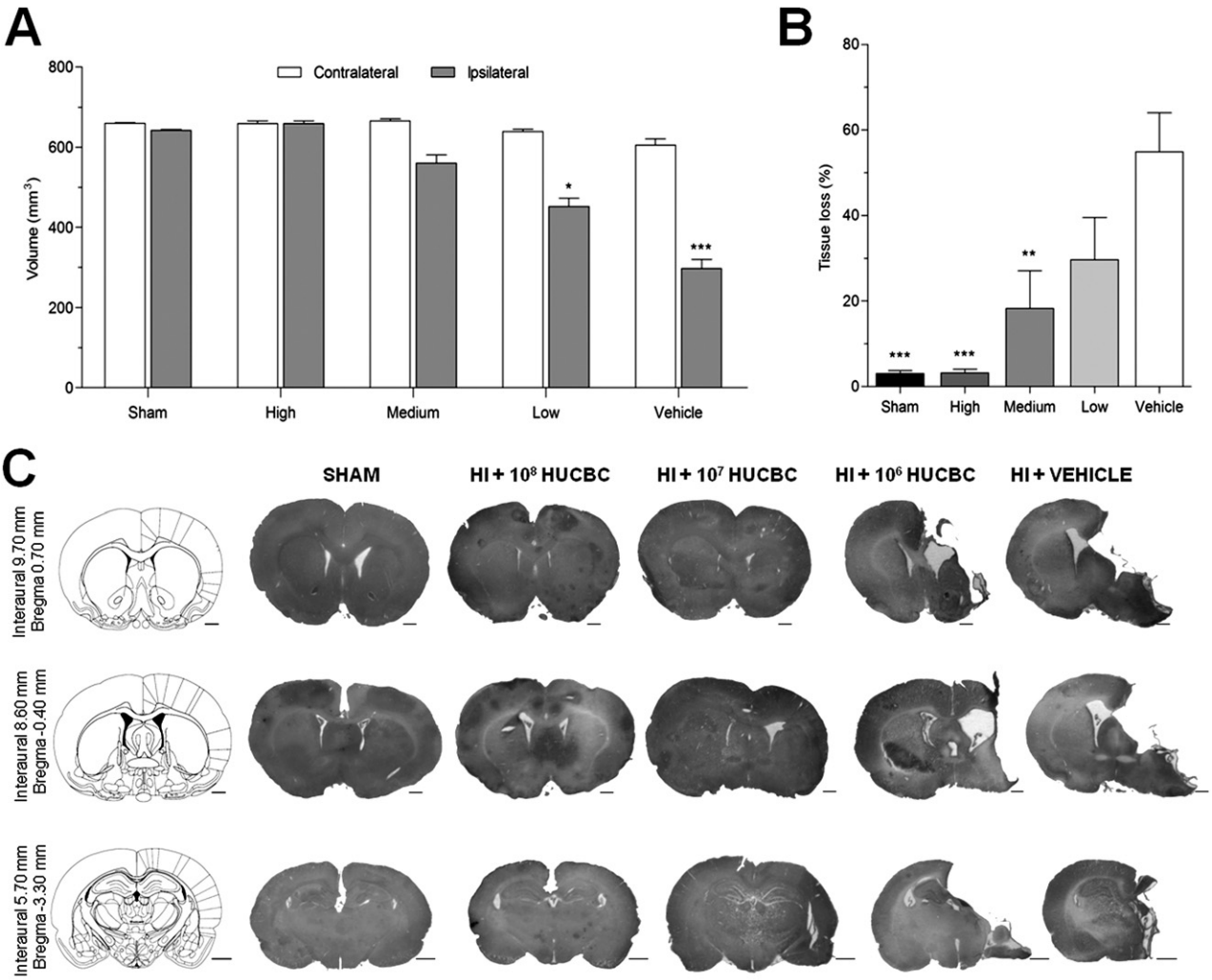

Fig. 3. HUCBC dose-dependently protect against brain atrophy in rats subjected to neonatal hypoxia-ischemia. (A) Absolute volumes of brain hemispheres are shown. The rats in the HI+vehicle and HI+low dose of HUCBC groups showed a significant decrease in the right hemispheric volume compared with the left. There was no difference between the hemispheric volumes in the medium- and high-dose HI animals. The values were presented as the mean±SEM; $n=10$ per group. Differences were analyzed by one-way ANOVA followed by the Bonferroni post hoc test; * $P<0.05$; *** $P<0.001$ vs. the left hemisphere. (B) Percentage of brain tissue loss is shown in a graph. When compared with sham-operated rats, the HI+vehicle group showed marked brain atrophy that was significantly lower in the medium- and high-dose HUCBC groups, suggesting a relationship between cell dosage and brain damage rescue. There was no statistically significant difference between the HI+vehicle and the HI+low-dose group. All values represent the mean±SEM; $n=10$ per group. ** $P<0.01$, and *** $P<0.001$ vs. the HI+vehicle group using Dunnett's multiple comparison post hoc test after one-way ANOVA. (C) Digitized images of coronal sections of the rat brains were stained using the Nissl procedure. The first column shows schematic drawings obtained from Paxinos and Watson's atlas. The slices show visible ipsilateral cortical atrophy (right hemisphere) in the HI+vehicle group that was attenuated at the highest doses of HUCBC. Calibration bars=1 mm.

pocampus of both hemispheres (Fig. 5A, B). Confocal photomicrographs with orthogonal reconstruction of grafted cells (Fig. 5C) revealed merged images of $HuNu^+$ cells and DAPI in brain parenchyma of all analyzed 7 days after transplantation. To confirm the migration of the delivered cells, we performed nested PCR analysis in seven animals using complementary primers to the human β-globin sequence 7 days after HUCBC transplantation. The expression of the band corresponding to the human gene was detected in the ipsilateral and contralateral hemispheres of six rats that received HUCBC via the jugular vein (Fig. 5D). The observations made from immunofluorescence staining and PCR analysis were consistent for all doses.

DISCUSSION

The neonatal HI rodent model produces long-term cognitive deficits and severe brain atrophy. We found that after a high dose of HUCBC (1×10^8 cells) transplanted intravenously, the rats demonstrated a significant attenuation of HI-induced spatial memory impairment 8 weeks after the treatment. Furthermore, medium (1×10^7 cells) and transplantation of high-doses of cells hindered the brain lesions caused by HI, which was not observed in low-dose- (1×10^6 cells) treated animals. In addition, HUCBC were identified in host rat brains 7 days after intravenous administration using immunofluorescence and PCR analysis.

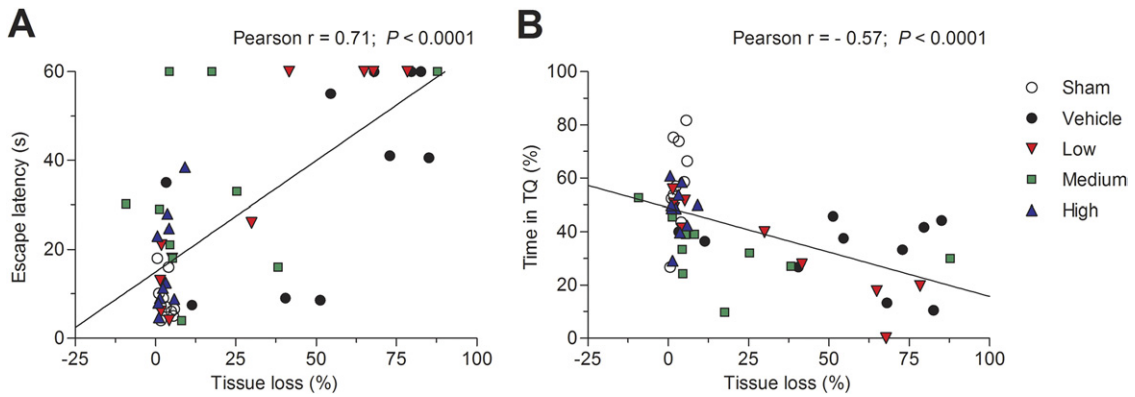

Fig. 4. Correlation of the degree of hemispheric tissue volume loss with spatial learning and memory in HI rats after HUCBC transplantation. (A) Correlation of the degree of hemispheric tissue volume loss and the escape latency of the MWM probe trial ($R=0.71$, $P<0.0001$). (B) Correlation of the degree of hemispheric tissue volume loss and the time spent in the target quadrant of the MWM probe trial ($R=-0.57$, $P<0.0001$). All experimental groups were pooled for both correlation analyses. For interpretation of the references to color in this figure legend, the reader is referred to the Web version of this article.

To investigate cognitive function after HUCBC transplantation, we performed the MWM test, which is an important measure of hippocampal-dependent spatial learning and memory after brain injuries, such as neonatal HI (Golan and Huleihel, 2006). Using this tool, our study revealed that injured animals treated with low and medium doses of HUCBC did not have a reduction of behavioral deficits. These results support our previous investigation that failed to show significant benefits in behavior performance 3 weeks after administration of 1×10^7 HUCBC (medium dose) in HI rats (de Paula et al., 2009). However, in the current report, the spatial learning and memory of HI animals treated with a high dose of HUCBC was significantly rescued compared with HI+vehicle animals 8 weeks after treatment. Only a few studies have addressed the effects of cellular therapy on the cognitive consequences after neonatal brain damage (Katsuragi et al., 2005; Ma et al., 2007). Consistent with our data, Ma et al (2007) reported that stem cells were effective in reducing behavioral impairments caused by HI, 2 and 8 months after cell transplantation. In addition to functional restoration in the MWM test, the authors also observed a neuropathological recovery in stem cell-treated animals (Ma et al., 2007).

In the current investigation, we observed that both medium and high doses of HUCBC provided significant brain damage repair after HI, in contrast to our previous data (de Paula et al., 2009). This discrepancy might be owing to the length of time that was chosen to assess neuronal injury changes. As previously shown in adult rats with ischemic lesions, no beneficial tissue effect of mesenchymal stem cell treatment was observed 29 days after the treatment. However, the authors found a statistically significant decrease in the lesion size in treated animals when evaluated 60 days post-transplantation (Kranz et al., 2010). In addition, we emphasize that, despite the brain tissue regeneration presented here, 1×10^7 HUCBC (medium dose) were not enough to mediate functional recovery after neonatal HI injury.

Although basic research has shown promising results in the field of cell-based therapy for neonatal brain injury (de Paula et al., 2010), the optimal dose for intravenous administration of stem cells has not yet been determined. According to a recent meta-analysis on intravenous stem cell delivery, there is a dose-response association between the number of stem cells injected and the functional effects of the treatment in experimental neurological diseases (Janowski et al., 2010). A pioneer study demonstrated that neural stem cells dose-dependently improved functional outcomes when transplanted into the ischemia-damaged striatum of rats (Saporta et al., 1999). In addition, Stroemer et al. (2009) observed that neural stem cell transplantation in rats after stroke promoted significant sensorimotor recovery depending on cell dosage (Stroemer et al., 2009). In line with our study, Yang et al. (2011) demonstrated that the highest doses of bone marrow mononuclear cells led to reduced lesion size and better functional performance in an animal model of stroke (Yang et al., 2011). The authors of these investigations observed discrete cell survival in the majority of the high-dose-treated animals, proposing a neuroprotective paracrine trophic mechanism.

Multiple mechanisms have been proposed to explain the promising behavioral and morphological outcomes observed in cell transplantation reports. However, the specific mechanisms of action responsible for the successful stem cell transplantation in HI brain injury have not yet been fully elucidated. It has been suggested that HUCBC treatment decreases brain damage and consequently improves neurological deficits, mainly by enhancing paracrine repair processes (Luo, 2011). It is possible that stem cells might serve as vehicles for specific molecules, acting as vectors for the production and/or release of neurotrophic factors. Consistent with *in vitro* studies (Arien-Zakay et al., 2009) and investigations using adult rats in a stroke model (Li et al., 2002), Yasuhara et al. (2010) reported an increase in GDNF, NGF, and BDNF brain levels in HI rats 3 days post-HUCBC transplantation (Ya-

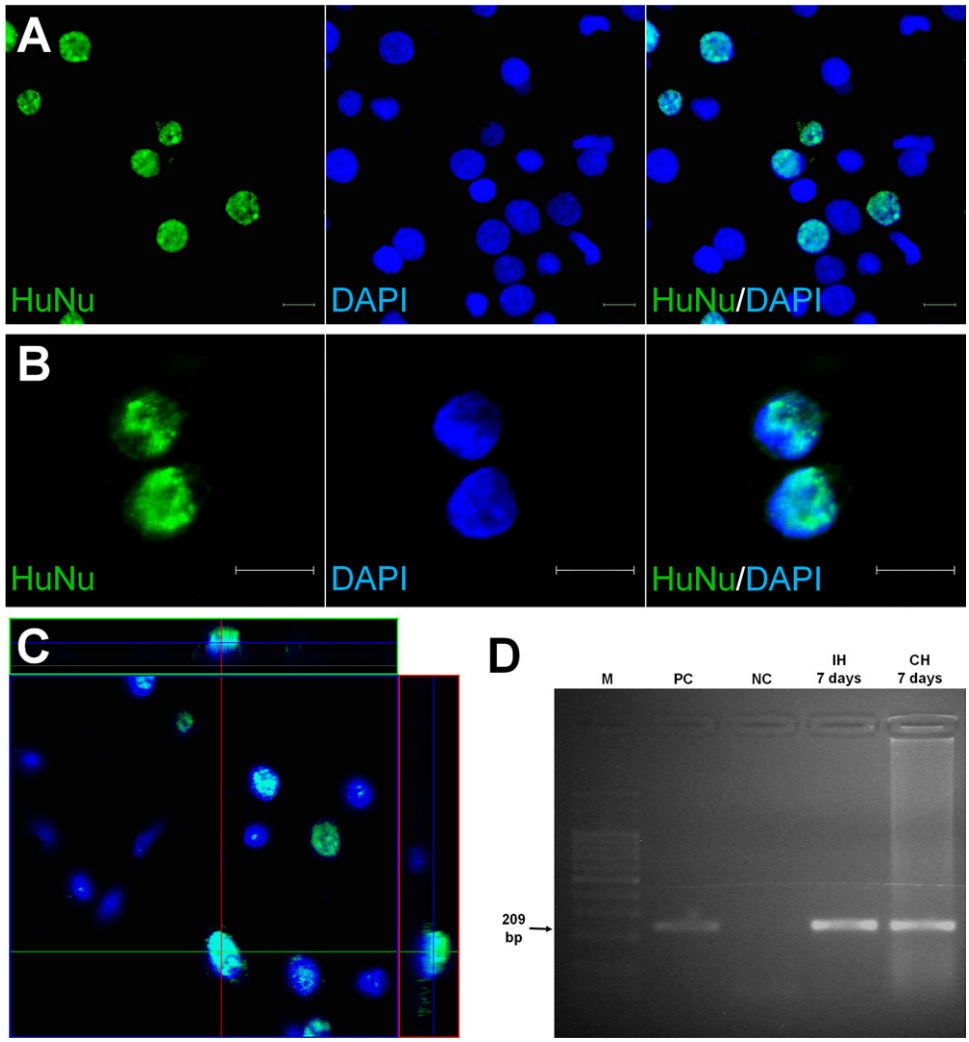

Fig. 5. Evidence of surviving HUCBC in a rat brain 7 d after a high dose of intravenous cell transplantation. Laser scanning fluorescent imaging of double-labeled cells and three-dimensional image reconstruction revealed that $HuNu^+$ cells (Alexa 488, green) were colocalized with DAPI (blue). (A) The individual channels and their merged image clearly demonstrate the colocalization of DAPI and HuNu in the HI rat cortex ipsilateral to the lesion. (B) $HuNu^+$ cells in the graft are shown at higher magnification in left hemisphere. The co-labeling of DAPI and $HuNu^+$ cells was highly cell-type specific. (C) Representative orthogonal images showing the colocalization of $HuNu^+$ cells and DAPI are presented. Red and green lines indicate corresponding points in the orthogonal planes, confirming the localization of the labeling within the cell after the summation of serial optical sections. (D) PCR analysis was performed to identify human cells in the rat brain. An agarose gel shows the presence of a band corresponding to the human β-globin gene sequence in the ipsilateral and contralateral hemispheres. Positive control (PC); negative control (NC); ipsilateral hemisphere (IH); contralateral hemisphere (CH). Calibration bars = 10 μm. For interpretation of the references to color in this figure legend, the reader is referred to the Web version of this article.

suhara et al., 2010). Neurotrophic support may also be responsible for axonal sprouting and consequently rescue behavior. Using neuroanatomical tracing, Daadi et al. (2010) demonstrated significant contralesional sprouting in HI rats after neural stem cell transplantation (Daadi et al., 2010). Additionally, some studies have reported that the functional benefits of mononuclear cord blood are related to an increase in endogenous neurogenesis. Bachstetter et al. (2008) demonstrated that intravenous administration of the mononuclear fraction of umbilical cord blood stimulates neurogenesis in the brains of aged rats (Bachstetter et al., 2008). Some authors have also suggested that transplanted cord mononuclear cells have the ability to modulate the post-injury inflammatory response thus facilitating the process of endogenous neurogenesis (Vendrame et al., 2005). Another important action mechanism that needed to be considered is that a high dose of HUCBC used in our study may have enhanced the blood vessel formation in ischemic areas. As demonstrated by Ramos et al. (2010), human cord blood is a source of endothelial, myeloid, and lymphoid precursors. The endothelial cells generated from common progenitors for the hematopoietic and vascular lineages in cord blood mononuclear cell fraction may be able to participate in new blood vessel formation (Ramos et al., 2010). However, more studies are needed to confirm these suggested mechanisms.

In the present study, we detected double-labeled $HuNu^+$ cells 7 days after cell transplantation. Most of the

HUCBC were widely dispersed throughout the cortical regions and other structures of both hemispheres. In addition, PCR analysis performed 7 days after HUCBC transplantation showed the presence of human β-globin in the rat brains. Recently, it has been shown that stem cells rapidly migrate to the lesion site within 4–10 days post-transplantation in a rat model of HI (Obenaus et al., 2011). Stromal cell-derived factor-1 (SDF-1) has been reported to be an important player in the recruitment and homing of transplanted HUCBC-derived mononuclear cells to the site of the HI brain lesion in newborn rats (Rosenkranz et al., 2010).

Translation of the experimental knowledge to human trials using cell-based therapy should consider important factors to bridge this gap. The optimization of the cell dose, route and devices for cellular delivery, selection of the optimal cell donor, timing of administration, and use of associated interventions are fundamental issues that should be addressed in the laboratory. As recommended by the Stem cell Therapeutics as an Emerging Paradigm in Stroke (STEPS) (Savitz et al., 2011) and Baby STEPS guidelines (Borlongan and Weiss, 2011), the experimental design for restorative therapies should include a cell dose-response study to reveal not only the optimal therapeutic dose, but also the maximum tolerable dose. With these considerations in mind, we demonstrated that a single intravenous transplantation of HUCBC dose-dependently hinders brain damage and spatial memory deficits in neonatal HI. Although only the high dose (1×10^8 HUCBC) promoted robust tissue neuroprotection and cognitive improvement, it may be interesting to test repeated dosing regimen. Some clinical studies have indicated that transplants using two cord blood units in hematological disease are feasible and may increase the applicability of grafts with a high cell dose. The authors also suggested that techniques such as *ex vivo* cell expansion may provide a good alternative to clinical use of high doses of HUCBC transplantation (Stanevsky et al., 2010; Ballen et al., in press; Kindwall-Keller et al., in press).

Today, four clinical trials promise relevant data on the therapeutic use of umbilical cord blood transplantations in pediatric patients with HI (phase I study at Duke University, NCT00593242) and cerebral palsy (phase II study at Duke University, NCT01147653; phases I and II at Georgia Health Sciences University, NCT01072370; phase I study at Sung Kwang Medical Foundation, NCT01193660). The cellular dosing regimen varies from 1 to 5×10^7 cells/kg, which is similar to human dose recommended for hematological diseases in infants but smaller than high-dose cell transplantation used in our study in rats weighting approximately 20 g. Although the use of 1×10^8 HUCBC dose may be difficult in the clinical setting because of the large number of cells needed, we suggest that our results may support clinical trials using high doses of cord blood cells taking into consideration three important factors presented here: (1) neonate rats tolerated well the high dose of human cells without specific side effects such as tumorigenicity or embolism; (2) a proper human umbilical cord blood collection provided a high dose of mononuclear cells ($\geq1\times10^8$) for transplantation in newborn rats; and (3) there was a strong relationship between cell dosage, brain damage regeneration, and impaired behavior recovery in HI. Finally, we emphasize that the outcomes of further clinical trials with a careful selection of homogeneous patients will determine whether high doses of HUCBC transplantation are clinically feasible and safe. Then, we could verify whether the benefits of HUCBC transplantation correspond to the expectations observed on experimental scenario.

CONCLUSIONS

To our knowledge, this is the first study to demonstrate that acute intravenous administration of HUCBC exerts a dose-dependent effect on long-term behavior and morphological outcomes in HI-injured rats. Thus, these results bring us closer to the clinical applications of cell-based therapy in neonatal HI. In summary, our current study reveals the therapeutic dose (1×10^8 mononuclear cells) necessary to promote robust tissue neuroprotection and stable functional improvement. We emphasize that dosage is an important factor in optimizing cellular transplantation. However, other questions as to the follow-up time required for neuroprotection and the additional action mechanisms demand further investigations, as these are essential tools for the translation of basic science to safe and effective clinical therapies after neonatal brain damage.

Acknowledgments—This work was supported by grants from Coordenação de Aperfeiçoamento de Pessoal de Nível Superior (CAPES), Pontifícia Universidade Católica do Rio Grande do Sul (PUCRS), Hemo Cord Clínica Médica Sociedade Simples Ltda., and Pandurata Ltda. Jaderson C. DaCosta is a researcher at Conselho Nacional de Desenvolvimento Científico e Tecnológico (CNPq). Simone de Paula and Samuel Greggio are the recipients of scholarships from CAPES and CNPq, respectively. The authors would like to thank professors Iván Izquierdo and Martín Cammarota for providing excellent research facility for our study at Centro de Memória (Instituto do Cérebro, PUCRS). The authors also thank Gianina Teribele Venturin for critical reading of the manuscript.

REFERENCES

Alles YC, Greggio S, Alles RM, Azevedo PN, Xavier LL, DaCosta JC (2010) A novel preclinical rodent model of collagenase-induced germinal matrix/intraventricular hemorrhage. Brain Res 1356: 130–138.

Arien-Zakay H, Lecht S, Bercu MM, Tabakman R, Kohen R, Galski H, Nagler A, Lazarovici P (2009) Neuroprotection by cord blood neural progenitors involves antioxidants, neurotrophic and angiogenic factors. Exp Neurol 216:83–94.

Bachstetter AD, Pabon MM, Cole MJ, Hudson CE, Sanberg PR, Willing AE, Bickford PC, Gemma C (2008) Peripheral injection of human umbilical cord blood stimulates neurogenesis in the aged rat brain. BMC Neurosci 9:22.

Ballen KK, Klein JP, Pedersen TL, Bhatla D, Duerst R, Kurtzberg J, Lazarus HM, Lemaistre CF, McCarthy P, Mehta P, Palmer J, Setterholm M, Wingard JR, Joffe S, Parsons SK, Switzer GE, Lee SJ, Rizzo JD, Majhail NS (in press) Relationship of race/ethnicity and survival after single umbilical cord blood transplantation for adults and children with leukemia and myelodysplastic syndromes. Biol Blood Marrow Transplant.

Bliss T, Guzman R, Daadi M, Steinberg GK (2007) Cell transplantation therapy for stroke. Stroke 38:817–826.

Borlongan CV, Weiss MD (2011) Baby: STEPS: a giant leap for cell therapy in neonatal brain injury. Pediatr Res 70:3–9.

Daadi MM, Davis AS, Arac A, Li Z, Maag AL, Bhatnagar R, Jiang K, Sun G, Wu JC, Steinberg GK (2010) Human neural stem cell grafts modify microglial response and enhance axonal sprouting in neonatal hypoxic-ischemic brain injury. Stroke 41:516–523.

de Paula S, Greggio S, DaCosta JC (2010) Use of stem cells in perinatal asphyxia: from bench to bedside. J Pediatr (Rio J) 86:451–464.

de Paula S, Vitola AS, Greggio S, de Paula D, Mello PB, Lubianca JM, Xavier LL, Fiori HH, Dacosta JC (2009) Hemispheric brain injury and behavioral deficits induced by severe neonatal hypoxia-ischemia in rats are not attenuated by intravenous administration of human umbilical cord blood cells. Pediatr Res 65:631–635.

Ferriero DM (2004) Neonatal brain injury. N Engl J Med 351: 1985–1995.

Galvin KA, Oorschot DE (2003) Continuous low-dose treatment with brain-derived neurotrophic factor or neurotrophin-3 protects striatal medium spiny neurons from mild neonatal hypoxia/ischemia: a stereological study. Neuroscience 118:1023–1032.

Garbuzova-Davis S, Sanberg CD, Kuzmin-Nichols N, Willing AE, Gemma C, Bickford PC, Miller C, Rossi R, Sanberg PR (2008) Human umbilical cord blood treatment in a mouse model of ALS: optimization of cell dose. PLoS ONE 3:e2494.

Golan H, Huleihel M (2006) The effect of prenatal hypoxia on brain development: short- and long-term consequences demonstrated in rodent models. Dev Sci 9:338–349.

Greggio S, de Paula S, de Oliveira IM, Trindade C, Rosa RM, Henriques JA, Dacosta JC (2011) NAP prevents acute cerebral oxidative stress and protects against long-term brain injury and cognitive impairment in a model of neonatal hypoxia-ischemia. Neurobiol Dis 44:152–159.

Harris DT (2008) Cord blood stem cells: a review of potential neurological applications. Stem Cell Rev 4:269–274.

Isola J, DeVries S, Chu L, Ghazvini S, Waldman F (1994) Analysis of changes in DNA sequence copy number by comparative genomic hybridization in archival paraffin-embedded tumor samples. Am J Pathol 145:1301–1308.

Iwasaki H, Kawamoto A, Ishikawa M, Oyamada A, Nakamori S, Nishimura H, Sadamoto K, Horii M, Matsumoto T, Murasawa S, Shibata T, Suehiro S, Asahara T (2006) Dose-dependent contribution of CD34-positive cell transplantation to concurrent vasculogenesis and cardiomyogenesis for functional regenerative recovery after myocardial infarction. Circulation 113:1311–1325.

Janowski M, Walczak P, Date I (2010) Intravenous route of cell delivery for treatment of neurological disorders: a meta-analysis of preclinical results. Stem Cells Dev 19:5–16.

Johnston MV, Fatemi A, Wilson MA, Northington F (2011) Treatment advances in neonatal neuroprotection and neurointensive care. Lancet Neurol 10:372–382.

Katsuragi S, Ikeda T, Date I, Shingo T, Yasuhara T, Mishima K, Aoo N, Harada K, Egashira N, Iwasaki K, Fujiwara M, Ikenoue T (2005) Implantation of encapsulated glial cell line-derived neurotrophic factor-secreting cells prevents long-lasting learning impairment following neonatal hypoxic-ischemic brain insult in rats. Am J Obstet Gynecol 192:1028–1037.

Kindwall-Keller TL, Hegerfeldt Y, Meyerson HJ, Margevicius S, Fu P, van Heeckeren W, Lazarus HM, Cooper BW, Gerson SL, Barr P, Tse WW, Curtis C, Fanning LR, Creger RJ, Carlson-Barko JM, Laughlin MJ (in press) Prospective study of one-vs two-unit umbilical cord blood transplantation following reduced intensity conditioning in adults with hematological malignancies. Bone Marrow Transplant.

Kranz A, Wagner DC, Kamprad M, Scholz M, Schmidt UR, Nitzsche F, Aberman Z, Emmrich F, Riegelsberger UM, Boltze J (2010) Transplantation of placenta-derived mesenchymal stromal cells upon experimental stroke in rats. Brain Res 1315:128–136.

Li Y, Chen J, Chen XG, Wang L, Gautam S, Xu Y, Katakowski M, Zhang L, Lu M, Janakiraman N, Chopp M (2002) Human marrow stromal cell therapy for stroke in rat: neurotrophins and functional recovery. Neurology 59:514–523.

Liao Y, Geyer MB, Yang AJ, Cairo MS (2011) Cord blood transplantation and stem cell regenerative potential. Exp Hematol 39:393–412.

Luo Y (2011) Cell-based therapy for stroke. J Neural Transm 118:61–74.

Ma J, Wang Y, Yang J, Yang M, Chang KA, Zhang L, Jiang F, Li Y, Zhang Z, Heo C, Suh YH (2007) Treatment of hypoxic-ischemic encephalopathy in mouse by transplantation of embryonic stem cell-derived cells. Neurochem Int 51:57–65.

Mayani H, Lansdorp PM (1998) Biology of human umbilical cord blood-derived hematopoietic stem/progenitor cells. Stem Cells 16:153–165.

Meier C, Middelanis J, Wasielewski B, Neuhoff S, Roth-Haerer A, Gantert M, Dinse HR, Dermietzel R, Jensen A (2006) Spastic paresis after perinatal brain damage in rats is reduced by human cord blood mononuclear cells. Pediatr Res 59:244–249.

Obenaus A, Dilmac N, Tone B, Tian HR, Hartman R, Digicaylioglu M, Snyder EY, Ashwal S (2011) Long-term magnetic resonance imaging of stem cells in neonatal ischemic injury. Ann Neurol 69:282–291.

Omori Y, Honmou O, Harada K, Suzuki J, Houkin K, Kocsis JD (2008) Optimization of a therapeutic protocol for intravenous injection of human mesenchymal stem cells after cerebral ischemia in adult rats. Brain Res 1236:30–38.

Park DH, Borlongan CV, Willing AE, Eve DJ, Cruz LE, Sanberg CD, Chung YG, Sanberg PR (2009) Human umbilical cord blood cell grafts for brain ischemia. Cell Transplant 18:985–998.

Paxinos G, Watson C (1986) The rat brain in stereotaxic coordinates. Sydney: Academic Press.

Pimentel-Coelho PM, Magalhaes ES, Lopes LM, Deazevedo LC, Santiago MF, Mendez-Otero R (2009) Human cord blood transplantation in a neonatal rat model of hypoxic-ischemic brain damage: functional outcome related to neuroprotection in the striatum. Stem Cells Dev 19:351–358.

Ramos AL, Darabi R, Akbarloo N, Borges L, Catanese J, Dineen SP, Brekken RA, Perlingeiro RC (2010) Clonal analysis reveals a common progenitor for endothelial, myeloid, and lymphoid precursors in umbilical cord blood. Circ Res 107:1460–1469.

Rice JE, Vannucci RC, Brierley JB (1981) The influence of immaturity on hypoxic-ischemic brain damage in the rat. Ann Neurol 9:131–141.

Rosenkranz K, Kumbruch S, Lebermann K, Marschner K, Jensen A, Dermietzel R, Meier C (2010) The chemokine SDF-1/CXCL12 contributes to the "homing" of umbilical cord blood cells to a hypoxic-ischemic lesion in the rat brain. J Neurosci Res 88:1223–1233.

Ruhil S, Kumar V, Rathee P (2009) Umbilical cord stem cell: an overview. Curr Pharm Biotechnol 10:327–334.

Sahni R, Sanocka UM (2008) Hypothermia for hypoxic-ischemic encephalopathy. Clin Perinatol 35:717–734, vi

Santner-Nanan B, Peek MJ, McCullagh P, Nanan R (2005) Therapeutic potential of stem cells in perinatal medicine. Aust N Z J Obstet Gynaecol 45:102–107.

Saporta S, Borlongan CV, Sanberg PR (1999) Neural transplantation of human neuroteratocarcinoma (hNT) neurons into ischemic rats. A quantitative dose-response analysis of cell survival and behavioral recovery. Neuroscience 91:519–525.

Savitz SI, Chopp M, Deans R, Carmichael ST, Phinney D, Wechsler L (2011) Stem cell therapy as an emerging paradigm for stroke (STEPS) II. Stroke 42:825–829.

Stanevsky A, Shimoni A, Yerushalmi R, Nagler A (2010) Double umbilical cord blood transplant: more than a cell dose? Leuk Lymphoma 51:975–982.

Stroemer P, Patel S, Hope A, Oliveira C, Pollock K, Sinden J (2009) The neural stem cell line CTX0E03 promotes behavioral recovery and endogenous neurogenesis after experimental stroke in a Dose-Dependent fashion. Neurorehabil Neural Repair 23:895–909.

Vendrame M, Cassady J, Newcomb J, Butler T, Pennypacker KR, Zigova T, Sanberg CD, Sanberg PR, Willing AE (2004) Infusion of human umbilical cord blood cells in a rat model of stroke dose-dependently rescues behavioral deficits and reduces infarct volume. Stroke 35:2390–2395.

Vendrame M, Gemma C, de Mesquita D, Collier L, Bickford PC, Sanberg CD, Sanberg PR, Pennypacker KR, Willing AE (2005) Anti-inflammatory effects of human cord blood cells in a rat model of stroke. Stem Cells Dev 14:595–604.

Venturin GT, Greggio S, Marinowic DR, Zanirati G, Cammarota M, Machado DC, Dacosta JC (2011) Bone marrow mononuclear cells reduce seizure frequency and improve cognitive outcome in chronic epileptic rats. Life Sci 89:229–234.

Wechsler L, Steindler D, Borlongan C, Chopp M, Savitz S, Deans R, Caplan L, Hess D, Mays RW, Boltze J, Boncoraglio G, Borlongan CV, Caplan LR, Carmichael ST, Chopp M, Davidoff AW, Deans RJ, Fisher M, Hess DC, Kondziolka D, Mays RW, Norrving B, Parati E, Parent J, Reynolds BA, Gonzalez-Rothi LJ, Savitz S, Sanberg P, Schneider D, Sinden JD, Snyder E, Steinberg GK, Steindler D, Wechsler L, Weiss MD, Weiss S, Victor S, Zheng T (2009) Stem cell therapies as an emerging paradigm in stroke (STEPS): bridging basic and clinical science for cellular and neurogenic factor therapy in treating stroke. Stroke 40:510–515.

Wolf D, Reinhard A, Seckinger A, Katus HA, Kuecherer H, Hansen A (2009) Dose-dependent effects of intravenous allogeneic mesenchymal stem cells in the infarcted porcine heart. Stem Cells Dev 18:321–329.

Wyatt JS, Gluckman PD, Liu PY, Azzopardi D, Ballard R, Edwards AD, Ferriero DM, Polin RA, Robertson CM, Thoresen M, Whitelaw A, Gunn AJ (2007) Determinants of outcomes after head cooling for neonatal encephalopathy. Pediatrics 119:912–921.

Xia G, Hong X, Chen X, Lan F, Zhang G, Liao L (2010) Intracerebral transplantation of mesenchymal stem cells derived from human umbilical cord blood alleviates hypoxic ischemic brain injury in rat neonates. J Perinat Med 38:215–221.

Yang B, Strong R, Sharma S, Brenneman M, Mallikarjunarao K, Xi X, Grotta JC, Aronowski J, Savitz SI (2011) Therapeutic time window and dose response of autologous bone marrow mononuclear cells for ischemic stroke. J Neurosci Res 89:833–839.

Yasuhara T, Hara K, Maki M, Xu L, Yu G, Ali MM, Masuda T, Yu SJ, Bae EK, Hayashi T, Matsukawa N, Kaneko Y, Kuzmin-Nichols N, Ellovitch S, Cruz EL, Klasko SK, Sanberg CD, Sanberg PR, Borlongan CV (2010) Mannitol facilitates neurotrophic factor upregulation and behavioral recovery in neonatal hypoxic-ischemic rats with human umbilical cord blood grafts. J Cell Mol Med 14:914–921.

You Z, Yang J, Takahashi K, Yager PH, Kim HH, Qin T, Stahl GL, Ezekowitz RA, Carroll MC, Whalen MJ (2007) Reduced tissue damage and improved recovery of motor function after traumatic brain injury in mice deficient in complement component C4. J Cereb Blood Flow Metab 27:1954–1964.

(Accepted 2 March 2012)
(Available online 13 March 2012)